0013-7227/03/$15.00/0
Printed in U.S.A.

The Journal of Clinical Endocrinology & Metabolism 88(5):2318–2326

doi: 10.1210/jc.2002-021907

RAS Point Mutations and PAX8-PPARγ Rearrangement in Thyroid Tumors: Evidence for Distinct Molecular Pathways in Thyroid Follicular Carcinoma

MARINA N. NIKIFOROVA, ROY A. LYNCH, PAUL W. BIDDINGER, ERIK K. ALEXANDER, GERALD W. DORN II, GIOVANNI TALLINI, TODD G. KROLL, AND YURI E. NIKIFOROV

Department of Pathology and Laboratory Medicine (M.N.N., P.W.B., Y.E.N.) and Division of Cardiology (R.A.L., G.W.D.), University of Cincinnati, Cincinnati, Ohio 45267-0529; Department of Medicine (E.K.A.), Brigham and Women's Hospital, Boston, Massachusetts 02115; Department of Pathology (G.T.), Yale University School of Medicine, New Haven, Connecticut 06510; and Department of Pathology and Laboratory Medicine (T.G.K.), Emory University School of Medicine, Winship Cancer Institute, Atlanta, Georgia 30322

A series of 88 conventional follicular and Hürthle cell thyroid tumors were analyzed for *RAS* mutations and *PAX8-PPARγ* rearrangements using molecular methods and for galectin-3 and HBME-1 expression by immunohistochemistry. A novel LightCycler technology-based method was developed to detect point mutations in codons 12/13 and 61 of the *H-RAS*, *K-RAS*, and *N-RAS* genes. Forty-nine percent of conventional follicular carcinomas had *RAS* mutations, 36% had *PAX8-PPARγ* rearrangement, and only one (3%) had both. In follicular adenomas, 48% had *RAS* mutations, 4% had *PAX8-PPARγ* rearrangement, and 48% had neither. Follicular carcinomas with *PAX8-PPARγ* typically showed immunoreactivity for galectin-3 but not for HBME-1, tended to present at a younger patient age and be smaller size, and were almost always overtly invasive. In contrast, follicular carcinomas with *RAS* mutations most often displayed an HBME-1-positive/galectin-3-negative immunophenotype and were either minimally or overtly invasive. Hürthle cell tumors infrequently had *PAX8-PPARγ* rearrangement or *RAS* mutations. These results suggest that conventional follicular thyroid carcinomas develop through at least two distinct and virtually nonoverlapping molecular pathways initiated by either *RAS* point mutation or *PAX8-PPARγ* rearrangement. (*J Clin Endocrinol Metab* 88: 2318–2326, 2003)

FOLLICULAR THYROID TUMORS include conventional follicular carcinoma, Hürthle cell (oncocytic) carcinoma, and their benign counterparts, follicular adenoma and Hürthle cell (oncocytic) adenoma. Follicular cancers account for approximately 15% of all thyroid malignancies, with about two thirds being conventional and one third Hürthle cell types (1). Conventional follicular carcinomas virtually never involve regional lymph nodes and have distant metastases, most commonly to the lungs and bones (10–20% of cases). Hürthle cell carcinomas develop blood-borne metastases but also spread to regional lymph nodes.

Preoperative diagnosis of follicular tumors is difficult because adenomas and carcinomas share similar cytologic features. Only two reliable histologic criteria, capsular and vascular invasion, are known to detect malignancy before local invasion or metastases, but these can be evaluated only after surgical resection. In addition, some cellular hyperplastic nodules and follicular variants of papillary carcinoma may mimic follicular tumors in fine-needle aspiration (FNA) specimens. As a result, many follicular lesions diagnosed as indeterminate or suspicious by FNA cytology are referred for surgery when only a small fraction (8–17%) prove to be malignant (2).

Recently, galectin-3 and HBME-1 immunostains have been suggested to be helpful for preoperative diagnosis of follicular carcinomas. Galectin-3, a member of the β-galactosidase-binding lectin family, is reportedly up-regulated in thyroid malignant tumors and undetectable in normal thyroid tissue or benign lesions (3–6). HBME-1 antibody, generated against a suspension of malignant mesothelial cells, is reported to be a sensitive and specific marker of thyroid malignancy as well (7–9). Each of these markers is imperfect in separating benign and malignant thyroid lesions, and their specificity and sensitivity vary greatly in different series (10–12).

Follicular tumors have been known to harbor activating point mutations of the *RAS* genes. Three *RAS* genes, *H-RAS*, *K-RAS*, and *N-RAS*, encode highly related 21-kDa proteins located at the inner surface of the cell membrane and play a central role in the transduction of signals arising from tyrosine kinase and G protein-coupled receptors. *RAS* point mutations in thyroid and other human neoplasms occur typically in codons 12, 13, or 61, leading to constitutive activation of downstream signaling pathways. Somatic missense mutations in codons 12/13 and 61 of one of the three *RAS* genes have been found in 18–52% of follicular carcinomas (13–18) and 24–53% of follicular adenomas (13–16, 19). A much lower incidence has been reported in Hürthle cell tumors (15–25% of carcinomas and 0–4% of adenomas) (15, 20, 21).

Recently a *PAX8-PPARγ* gene fusion was identified in a significant portion of follicular carcinomas, some with a cytogenetically detectable translocation t(2;3)(q13;p25) (22). The t(2;3) rearrangement leads to an in-frame fusion of the *PAX8* gene, which encodes a paired domain transcription

Abbreviations: FMCA, Fluorescence melting curve analysis; FNA, fine-needle aspiration; PPAR, peroxisome proliferator-activated receptor; T_m, melting temperature.

factor, with the peroxisome proliferator-activated receptor (PPAR) γ gene. In the original report, *PAX8-PPARγ* fusion was detected in 63% of follicular carcinomas but not in follicular adenomas, papillary carcinomas, or nodular hyperplasias, suggesting that it may represent a specific molecular marker of follicular carcinomas (22). In recent follow-up series, *PAX8-PPARγ* was identified by RT-PCR in 26–56% of follicular carcinomas and in 0–13% of follicular adenomas, 0–3% of Hürthle cell carcinomas, and 0–1% papillary carcinomas (23–25). Chromosomal rearrangement is likely to be a preferable mechanism of *PPARγ* activation in thyroid tumors because no point mutations in the *PPARγ* gene were found in thyroid carcinomas and cell lines (26).

To date, the correlation between *PAX8-PPARγ* rearrangements and *RAS* point mutations in thyroid follicular tumors has not been studied. In the present study, we have analyzed the association between these genetic alterations and their correlation with galectin-3 and HBME-1 immunoreactivity.

Materials and Methods

Sample selection and tumor classification

We studied 88 thyroid tumors including 33 conventional follicular carcinomas, 23 conventional follicular adenomas, 19 Hürthle cell carcinomas, and 13 Hürthle cell adenomas. The tumor samples were collected from the Cincinnati University Hospital (48 samples), Brigham and Women's Hospital (16 samples), Yale New Haven Hospital (10 samples), or obtained through the Cooperative Human Tissue Network (CHTN) (14 samples). In 52 cases, snap-frozen tissue and in 36 cases paraffin-embedded tissue was available. The study was approved by the University of Cincinnati Institutional Review Board.

Tumors were classified according to widely accepted histologic criteria (27, 28). Briefly, tumors were diagnosed as Hürthle cell (oncocytic) neoplasms when more than 75% of cells had oncocytic features. Follicular and Hürthle cell carcinomas were distinguished from adenomas on the basis of invasion of the entire thickness of the tumor capsule and/or invasion of blood vessels within the capsule or immediately external to it. Adenomas were separated from hyperplastic nodules based on the presence of encapsulation, compression of the adjacent thyroid parenchyma, and uniform hypercellular appearance.

Histologically, follicular carcinomas are subdivided into minimally invasive and widely invasive (27, 28). For the purpose of this study, we subdivided follicular carcinomas into three groups according to degree invasiveness.

Minimally invasive. This is an encapsulated neoplasm with microscopically detectable one or two microscoric foci of capsular or vascular invasion. The major differential diagnosis for such cases is follicular adenoma, and distinction from adenoma is often difficult and requires deeper sectioning of suspicious areas.

Overtly invasive. These are completely or partially encapsulated tumors with multiple (at least three, typically more than five) areas of capsular and vascular invasion but still confined to the thyroid gland. Capsular invasion is typically seen as a broad-based extension through the tumor capsule, and endotheliolized tumor aggregates are usually found in several consecutive blood vessels. The diagnosis of follicular carcinoma in such cases is straightforward, although the tumor does not show extrathyroidal extension.

Widely invasive. Widely invasive neoplasm typically replaces the entire thyroid lobe, with extrathyroidal extension and invasion of perithyroidal tissues. The tumor lacks evidence of encapsulation. Diagnosis of malignancy is unequivocal, even on gross examination. Differential diagnosis includes poorly differentiated or anaplastic carcinoma.

Nucleic acid isolation and reverse transcription

DNA was extracted by the phenol-chloroform method as previously described (29). RNA isolation from snap-frozen and paraffin-embedded tissue was performed using Trizol reagent (Invitrogen, Carlsbad, CA) as previously described (30). Three micrograms total RNA extracted from frozen tissue and 5 μl RNA extracted from paraffin-embedded tissue were reverse transcribed in a volume of 20 μl, using random hexamer priming and Superscript II RT (Invitrogen) according to the manufacturer's protocol. All cDNA samples were tested to assess the adequacy of RNA by amplifying a 247-bp control sequence of the *PGK* gene as reported elsewhere (31).

Detection of RAS mutations

Point mutations in codons 12/13 and 61 of the *H-*, *K-*, and *N-RAS* genes were detected using three different methods.

LightCycler PCR and fluorescence melting curve analysis (FMCA). LightCycler technology has been demonstrated as an efficient method for detection of *N-RAS* mutations in human tumors (32, 33). It is based on rapid-cycle PCR amplification of the locus containing a mutational hot spot on the LightCycler (Roche Molecular Biochemicals, Manheim, Germany) using a hybridization probe format, followed by FMCA. This format requires a pair of primers and two fluorescently labeled oligonucleotide probes and relies on fluorescence resonance transfer interaction between two probes that hybridize adjacent to one another, so that one fluorophore functions as the donor and another as the acceptor, the latter emitting a light of specific wavelength (34). For the detection of a point mutation, one probe is designed to span the mutation site, and the products are distinguished based on their distinct melting temperatures (T_m), which reflect the thermodynamic stability of the perfectly complementary and mismatched probe-target duplexes.

For each mutational hot spot, a pair of primers and two internal oligonucleotide probes were obtained (Table 1). To detect *N-RAS* 12/13 and *N-RAS* 61 mutations, primers and probes were used as described by Elenitoba-Johnson *et al.* (32) with some modifications. Primers and probes for the other four hot spots were designed with the help of Olfert Landt, TIB Molbiol (Berlin, Germany). All primers and probes were obtained from TIB Molbiol. Amplification was performed in a glass capillary using 50–100 ng DNA in a 20-μl volume containing 2 μl of 10× LightCycler DNA master hybridization probes [containing PCR buffer, deoxynucleotide triphosphates, 10 mM $MgCl_2$, and Taq polymerase (Roche), 1.6 μl of 25 mM $MgCl_2$, 40 pmol of each primer, and 2 pmol of each hybridization probe]. The reaction mixture was subjected to 40 cycles of rapid PCR consisting of denaturation at 94 C for 1 sec, annealing at 50–54 C for 20 sec, and extension at 72 C for 10 sec. Postamplification FMCA was performed by gradual heating of samples at a rate of 0.2 C/sec from 45 C to 95 C. Fluorescence melting peaks were built by plotting of the negative derivative of fluorescent signal corresponding to the temperature (−dF/dT).

Normal placental DNA was used as a negative control and DNA from cell lines carrying one of the *RAS* mutations served as a positive control (29). All PCR products that showed deviation from the wild-type (placental DNA) melting peak were sequenced after purification through Microcon PCR kit (Millipore Corp., Billerica, MA) to verify the presence of *RAS* mutation and detect the exact nucleotide change.

DNA heteroduplex analysis by HPLC (WAVE HPLC). To detect *RAS* mutations using this method, 200 ng DNA from each sample were amplified using conventional PCR with primers flanking codons 12/13 and 61 of the three *RAS* genes. The PCR products (ranging in size from 182–400 bp) were then characterized by temperature-dependent denaturing HPLC on WAVE apparatus (Transgenomic, Inc., Omaha, NE) and eluted using a linear gradient (typically 10–20%) of acetonitrile in 0.1 M triethyl ammonium acetate over 7–10 min, as described previously (35). Optimal melting temperature and elution gradient acetonitrile programs for each PCR product were initially estimated using WAVEMaker 4.0 software (Transgenomic). Negative and positive controls were as described above. All samples that displayed a deviation from normal (placental DNA) elution profiles were directly sequenced.

Direct DNA sequencing. Two hundred nanograms of DNA were PCR amplified using primers and conditions reported previously (29) and direct sequenced using an automated ABI model 377 sequencer (Applied Biosystems, Foster City, CA). Both sense and antisense primers were used for sequencing to assure the detection of heterozygous mutations in the *RAS* genes.

TABLE 1. Primers and probes used for LightCycler amplification and FMCA

Mutational hot spot	Nucleotide sequence	Nucleotide position
N-RAS		
Codons 12/13	5′-GCT GGT GTG AAA TGA CTG AG-3′[a]	88938–88957[b]
	5′-GAT GAT CCG ACA AGT GAG AG-3′	89155–89096
	5′-TTG GAG CAG GTG GTG TTG-fluorescein-3′	88974–88991
	5′-LC-Red 640-GAA AAG CGC ACT GAC AAT CCA GCT AAT CCA GAA CCA-phosphate-3′	88993–89028
Codon 61	5′-CCT GTT TGT TGG ACA TAC TG-3′[a]	91168–91187[b]
	5′-CCT GTA GAG GTT AAT ATC CG-3′	91310–91291
	5′-CCT GTC CTC ATG TAT TGG TCT CTC ATG GCA CT-fluorescein-3′	91243–91212
	LC-Red 705-TAC TCT TCT TGT CCA GCT GT-phosphate-3′	91210–91191
H-RAS		
Codons 12/13	5′-TGA GGA GCG ATG ACG GAA-3′	1655–1672[c]
	5′-GCG CTA GGC TCA CCT CTA T-3′	1787–1769
	5′-AGC TGG ATG GTC AGC GCA CTC TTG CCC-fluorescein-3′	1731–1715
	5′-LC Red640-CAC CGC CGG CGC CCA C-phosphate-3′	1713–1688
Codon 61	5′-GTC CTC CTG CAG GAT TCC TA-3′	2030–2049[c]
	5′-ATG GCA AAC ACA CAC AGG AA-3′	2181–2162
	5′-GAT ACC GCC GGC CAG GAG GA-fluorescein-3′	2099–2118
	5′-LC Red640-TAC AGC GCCATG CGG GAC CAG T-phosphate-3′	2120–2141
K-RAS		
Codons 12/13	5′-AAG GCC TGC TGA AAA TGA CTG-3′	82–102[d]
	5′-GGT CCT GCA CCA GTA ATA TGC A-3′	246–225
	5′-CGT CCA CAA AAT GAT TCT GAA TTA GCT GTA TCG TCA AGG CAC T-fluorescein-3′	186–144
	5′-LC Red640-TGC CTA CGC CAC CAG CTC CAA-phosphate-3′	141–112
Codon 61	5′-AGG ATT CCT ACA GGA AGC AAG TAG-3′	356–379[e]
	5′-CCC TCC CCA GTC CTC ATG-3′	476–459
	5′-TGC ACT GTA CTC CTC TTG ACC TGC T-fluorescein-3′	444–420
	5′-LC Red705-TCG AGA ATA TCC AAG AGA CAG GTT TCT CCA-phosphate-3′	416–387

[a] N-RAS codons 12/13 and 61 design of primers and probes was as previously reported by Elenitoba-Johnson *et al.* (32) with some modifications.
[b] GenBank accession no. AL096773.
[c] GenBank accession no. J00277.
[d] GenBank accession no. L00045.
[e] GenBank accession no. L00046.

Detection of PAX8-PPARγ rearrangement

Most of the cases employed in this study were previously analyzed for *PAX8-PPARγ* rearrangement by RT-PCR (58 patients) (23) and *PPARγ* with 3p25 probe by fluorescence *in situ* hybridization (16 patients) (22, 25). Fourteen additional tumors were studied for *PAX8-PPARγ* fusion by RT-PCR as previously described (23). PCR products were resolved by electrophoresis in a 1.5% agarose gel and in selected cases sequenced using an automated ABI model 377 sequencer.

Immunohistochemical analysis

Immunostaining was performed on paraffin-embedded sections using avidine-streptavidin immunoperoxidase method with monoclonal antibodies against galectin-3 (Vector Laboratories Ltd., Burlingame, CA) at a dilution of 1:100 and HBME-1 (DAKO Corp., Carpinteria, CA) at a dilution of 1:80 on automated Benchmark system (Ventana Medical Systems, Inc., Tuscon, AZ). Antigen retrieval was achieved by incubation at mild degree in cell condition 1 solution (Ventana). Paraffin sections from a papillary thyroid carcinoma were used as a positive control. For galectin-3, staining was considered specific when cytoplasmic and/or nuclear reactivity was noted. For HBME-1, only membranous and apical/colloidal immunoreactivity was considered specific (9). For both antibodies, tumors were scored positive when more than 10% of cells were immunoreactive.

Results

RAS point mutations

First, DNA from 47 tumors, including 20 samples isolated from frozen tissue and 27 from paraffin-embedded tissue, and six cell lines with known *RAS* mutations were analyzed using LightCycler FMCA and WAVE HPLC. The detection of *RAS* mutations by both methods was compared with that by direct DNA sequencing as the gold standard. Nine thyroid tumors had *N-RAS* codon 61 mutations (7 CAA→CGA and 2 CAA→AAA) and another two cases had *H-RAS* codon 61 CAG→AAG mutation by sequencing. LightCycler FMCA identified *RAS* mutations in all 11 tumors and in all six cell lines with known *RAS* mutations (Fig. 1).

For WAVE HPLC, all 20 DNA samples extracted from fresh tissue were efficiently amplified by PCR and amendable to the analysis, whereas of 27 cases from paraffin-embedded tissue, 9–18 samples failed to amplify various *RAS* regions, probably because of a limited DNA quality and larger size of amplicons (182–400 bp). Nine informative cases revealed abnormal elution profiles, five of which corresponded to specific *RAS* mutations with another four having a codon 27 *H-RAS* polymorphism, as detected by sequencing. Among six informative cases with *RAS* mutations identified by direct sequencing, five (83%) were detected by WAVE HPLC (data not shown).

Taking into account that LightCycler FMCA was as sensitive and specific as direct sequencing and no new mutations were detected by WAVE HPLC, remaining tumor samples were analyzed for *RAS* mutations by LightCycler FMCA and sequencing of PCR products showing abnormal melting curves. Overall, *RAS* mutations were detected in 17 (52%) follicular carcinomas, 11 (48%) follicular adenomas, 2 (11%) Hürthle cell carcinomas, and 1 (8%) Hürthle cell adenoma

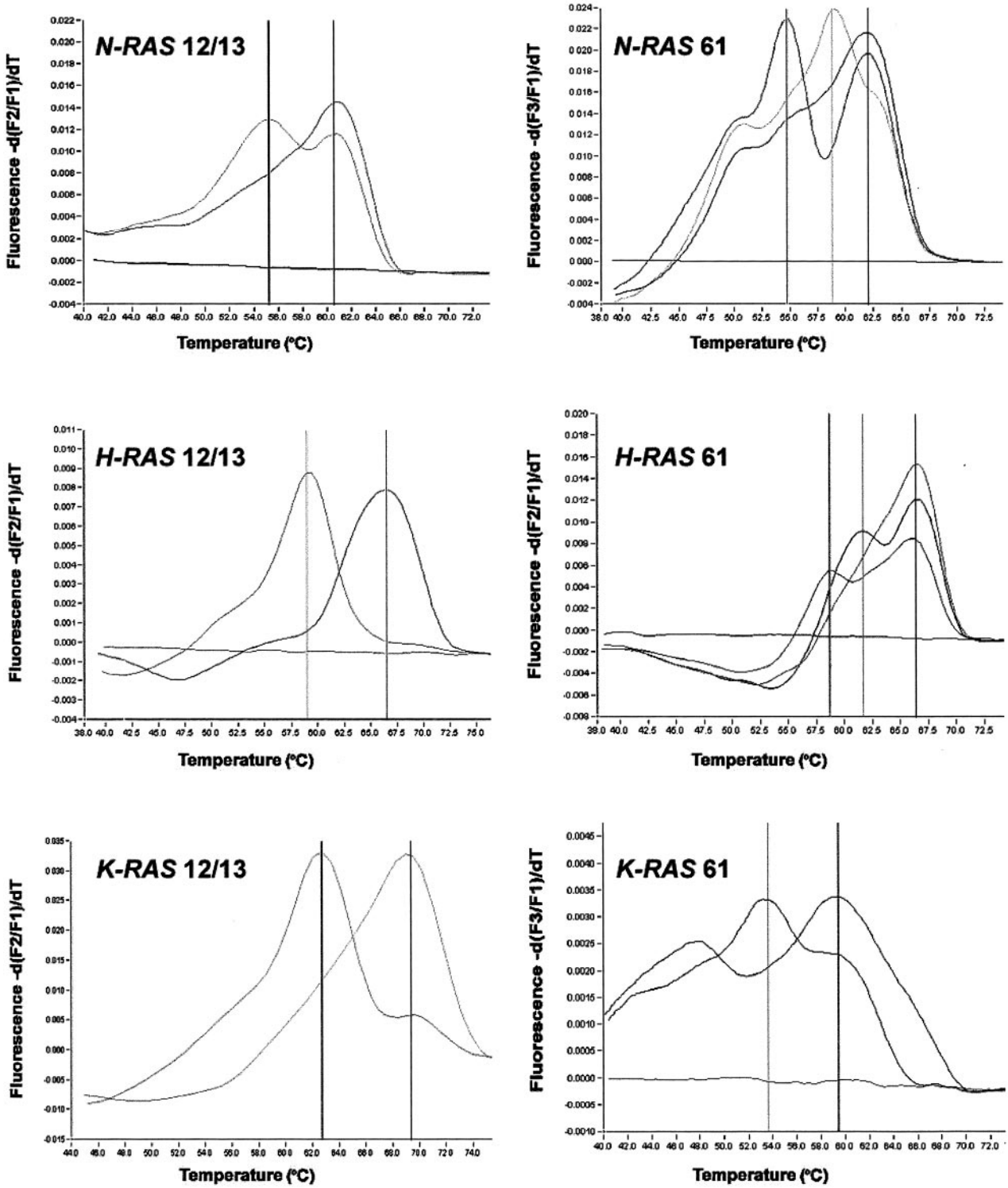

FIG. 1. LightCycler FMCA detection of *RAS* point mutations based on distinct T_m of duplexes formed between the wild-type probe and either wild-type (wt) or mutant sequences. For *N-RAS* 12/13 locus, the wt sequence T_m was 60.6 C and the GGT→TGT mutation T_m was 55.2 C. For *N-RAS* 61, the wt T_m was 62.1 C, the CAA→CGA mutation T_m was 58.8 C, and the CAA→AAA mutation T_m was 54.7 C. For *H-RAS* 12/13, the wt T_m was 66.6 C and the GGC→GTC mutation T_m was 59 C. For *H-RAS* 61, the wt T_m was 66.4 C, the CAG→CGG mutation T_m was 61.7 C, and the CAG→AAG mutation T_m was 58.8 C. For *K-RAS* 12/13, the wt T_m was 69.4 C and the GGT→GTT mutation T_m was 62.8 C. For *K-RAS* 61, the wt T_m was 59.5 C and the CAA→CAT mutation T_m was 53.6 C. All mutations shown were heterozygous because the products also demonstrated a wt peak, except for the homozygous *H-RAS* 12 GGC→GTC mutation in the T24 cell line.

(Table 2). In follicular carcinomas and adenomas, the CAA→CGA mutation of *N-RAS* codon 61 was the most common. In Hürthle cell tumors, mutations were observed only in *H-RAS* codon 61 and *K-RAS* codon 12. The overall spectrum of *RAS* mutation detected in these cases is shown in Table 3.

PPARγ rearrangement

Seventy-two tumors were studied for *PAX8-PPARγ* rearrangement by RT-PCR. The fusion was found in 5 of 17 follicular carcinomas, in 1 of 23 follicular adenomas, but not in 32 Hürthle cell tumors. Five tumors (four follicular carcinomas and one follicular adenoma) with *PAX8-PPARγ* rearrangement showed products consistent with fusion between exon 9 of *PAX8* and exon 1 of *PPARγ*. One other follicular carcinoma showed fusion between exon 7 of *PAX8* and exon 1 of *PPARγ*. Sixteen additional follicular carcinomas were selected for study based on rearrangement status by fluorescence *in situ* hybridization with 3p25 probes flanking the *PPARγ* gene. Eight follicular carcinomas were rearrangement positive, eight cases with rearrangement negative. The overall prevalence of *PPARγ* rearrangement in these tumors is summarized in Table 2.

Galectin-3 and HBME-1 immunohistochemistry

Thirty-three follicular carcinomas and 23 follicular adenomas were analyzed for galectin-3 and HBME-1 expression by immunohistochemistry (Fig. 2). Overall, 70% of follicular carcinomas and 30% of follicular adenomas showed immunoreactivity with at least one of the antibodies (Table 4). In general, immunoreactivity with both antibodies in the follicular tumors was more often focal than diffuse and of weaker intensity in comparison with those we typically observe in papillary carcinomas.

Correlation between RAS mutations and PPARγ rearrangement and galectin-3 and HBME-1 immunohistochemistry

Of 88 total tumors, 34% had only *RAS* mutations, 15% had only *PPARγ* rearrangement, and 1% had both. Among conventional follicular carcinomas, 49% had a *RAS+/PPARγ−* genotype and 36% had a *PPARγ+*/RAS− genotype. One follicular carcinoma (3%) harbored both mutations (Table 2). These genotypic changes were correlated with galectin-3 and HBME-1 immunohistochemistry within the same tumors. Follicular carcinomas with *PPARγ* rearrangement showed immunoreactivity for galectin-3 in 75% of cases and no immunoreactivity for HBME-1 in 59% of cases. In contrast, follicular carcinomas with *RAS* mutations were mostly negative for galectin-3 (88%) and positive for HBME-1 (62%) (Table 5).

Clinical-pathological features of tumor groups are summarized in Table 5. Follicular carcinomas with the *PPARγ+*/RAS− genotype had a tendency to develop in younger patients, be of a smaller size, and almost all of them were overtly invasive at presentation (Fig. 3). Follicular carcinomas with *RAS+/PPARγ−* genotype tended to present at older age, be larger in size, and show a wide range of invasiveness. Two tumors with focal areas of poorly differentiated histology were both *RAS+/PPARγ−*.

Discussion

We report here that 85% of conventional follicular thyroid carcinomas develop through two distinct and virtually nonoverlapping molecular pathways: one involving *RAS* point mutations and another involving *PAX8-PPARγ* rearrangement. The fact that only 1 of 33 follicular carcinomas had both mutations suggests at least two possibilities: These mutations involve activation of the same signaling pathway so that the occurrence of two mutations provides little additional growth advantage, or conventional follicular carcinomas consist of at least two groups of tumors developing through distinct molecular mechanisms. Our results obtained by immunohistochemistry support the second possibility because follicular carcinomas with *RAS* mutations were found typically to express HBME-1 and little galectin-3, whereas follicular carcinomas with *PPARγ* rearrangement characteristically expressed galectin-3 and less HBME-1. Potential differences were also observed in the clinical-pathological features in these two cancer groups. For example, tumors

TABLE 2. Prevalence of *RAS* point mutations and *PPARγ* rearrangement in conventional follicular and Hürthle cell tumors

	Follicular carcinomas (n = 33)	Follicular adenomas (n = 23)	Hürthle cell carcinomas (n = 19)	Hürthle cell adenomas (n = 13)
RAS+	16 (49%)[a]	11 (48%)	2 (11%)	1 (8%)
PAX8-PPARγ+	12 (36%)[a]	1 (4%)	0	0
PAX8-PPARγ+/RAS+	1 (3%)	0	0	0
−/−	4 (12%)	11 (48%)	17 (89%)	12 (92%)

[a] Not including one follicular carcinoma positive for both *RAS* and *PAX8-PPARγ*.

TABLE 3. Spectrum of *RAS* mutations identified in conventional follicular and Hürthle cell tumors

		Follicular carcinomas	Follicular adenomas	Hürthle cell carcinomas	Hürthle cell adenomas
N-RAS codon 61	CAA→CGA	12 (70%)	6 (55%)		
	CAA→AAA	2 (12%)	1 (9%)		
H-RAS codon 61	CAG→AAG	2 (12%)	2 (18%)		1 (100%)
	CAG→CGG	1 (6%)	2 (18%)	1 (50%)	
K-RAS codon 12	GGT→GAT			1 (50%)	
Total *RAS* mutations		17 (100%)	11 (100%)	2 (100%)	1 (100%)

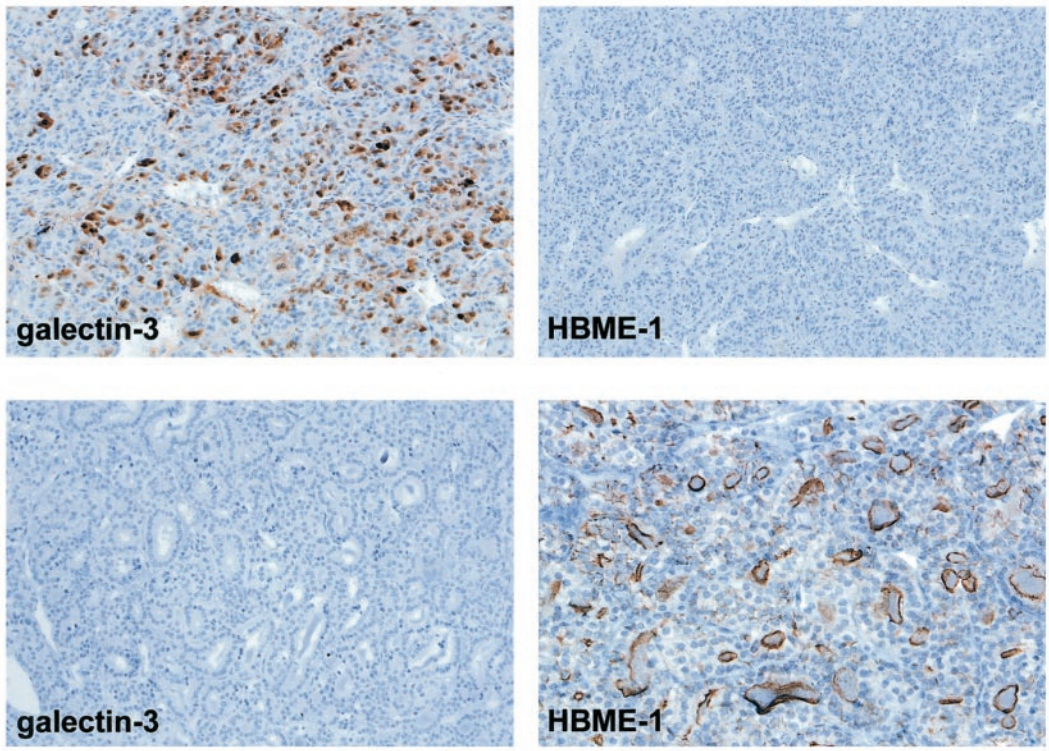

FIG. 2. Immunohistochemical analysis for galectin-3 and HBME-1. Gelactin-3 immunoreactivity was typically both cytoplasmic and nuclear, whereas specific HBME-1 immunoreactivity was membranous and apical/colloidal. Follicular carcinomas with the *PPARγ*+/RAS− genotype were commonly positive for galectin-3 and negative for HBME-1 (*top*), whereas tumors with the *RAS*+/*PPARγ*− genotype were typically negative for galectin-3 and positive for HBME-1 (*bottom*).

TABLE 4. Immunoreactivity for galectin-3 and HBME-1 in thyroid tumors

	Follicular carcinomas (n = 33)	Follicular adenomas (n = 23)
Galectin-3 only	5 (15%)	1 (4%)
HBME-1 only	11 (34%)	3 (13%)
Galectin-3/HBME-1	7 (21%)	3 (13%)
−/−	10 (30%)	16 (70%)

TABLE 5. Immunoprofiles and clinical-pathological features of follicular carcinomas with *PPARγ*+/*RAS*− and *RAS*+/*PPARγ*− genotypes

	PPARγ+/*RAS*− (n = 12)	*RAS*+/*PPARγ*− (n = 16)	*P*
Galectin-3/HBME-1			
+/−	5 (42%)	0	0.002
+/+	4 (33%)	2 (12%)	
−/+	1 (8%)	8 (50%)	0.05
−/−	2 (17%)	6 (38%)	
Age, average (range)	35.7 ± 11 yr (24–56 yr)	46.7 ± 20.3 yr (21–85 yr)	<0.1
F/M ratio	3/1	4/1	
Tumor size, average	3.6 ± 2.2 cm	5.0 ± 3.1 cm	<0.2
Predominant pattern			
Microfollicular	8 (67%)	11 (69%)	
Trabecular	3 (25%)	3 (19%)	
Solid	1 (8%)	0	
Normofollicular	0	2 (12%)	
Thick capsule	100%	86%	
Capsular invasion	100%	93%	
Vascular invasion	83%	85%	
Invasiveness			
Minimally invasive	1 (8%)	7 (44%)	0.1
Overtly invasive	11 (92%)	8 (50%)	0.05
Widely invasive	0	1 (6%)	
Foci of poorly differentiated carcinoma	0	2 (12%)	

with *PAX8-PPARγ* tended to present mostly during the fourth decade of life and be somewhat smaller in size, whereas *RAS*-positive tumors presented at older age, typically during the fifth decade of life, and were larger.

There was also significant variability in histologic invasiveness between tumors harboring *PAX8-PPARγ* and *RAS* mutations (Fig. 4). For example, 12 of 13 tumors with *PPARγ* rearrangement were follicular carcinomas, but only one was a follicular adenoma. Eleven of the 12 follicular carcinomas with *PAX8-PPARγ* were overtly invasive and demonstrated multifocal capsular and vascular invasion. The follicular adenoma had a thick capsule and displayed strong and diffuse HBME-1 and galectin-3 (carcinoma-like) immunoreactivity, raising the possibility it might be a preinvasive or *in situ* follicular carcinoma. Thus, it is likely that *PAX8-PPARγ* rearrangement confers invasive potential at the earliest tumor stages such that a benign follicular adenoma precursor lesion does not exist. High frequency of vascular invasion in these tumors correlates with the possibility of advanced disease, and distant metastases have been observed in follicular carcinomas with *PAX8-PPARγ* (36) (Dwight, T., and C. Larsson, personal communication; Kroll, T. G., unpublished data).

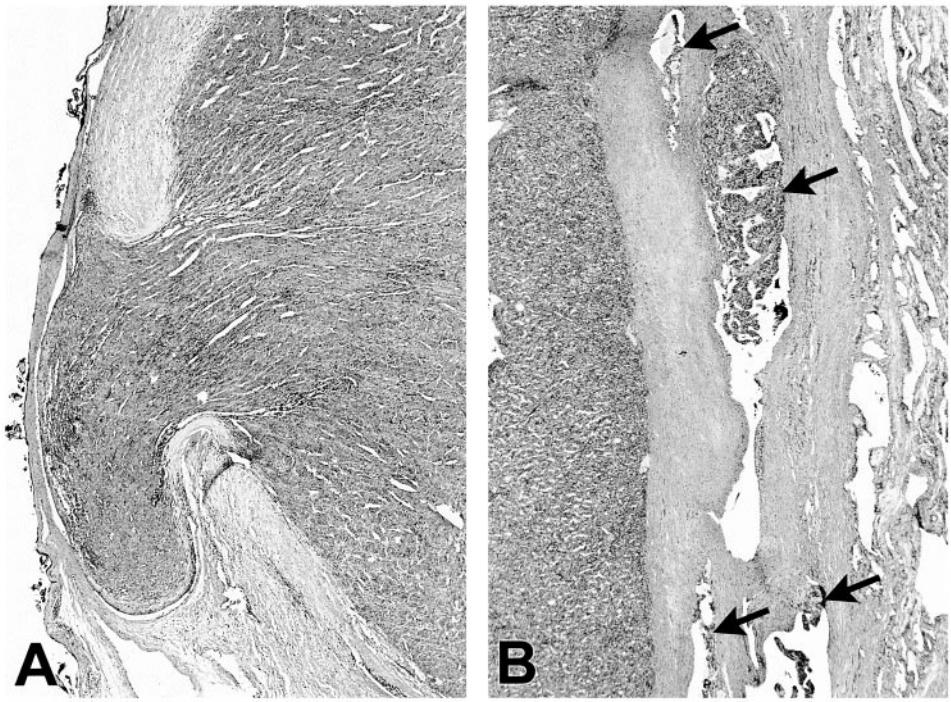

FIG. 3. Microscopic features of overtly invasive follicular carcinoma. A, Broad-based invasion through the tumor capsule. B, Multifocal vascular invasion with tumor thrombi identifiable in four consecutive blood vessels within the tumor capsule (*arrows*). Note that despite the readily identifiable features of invasive growth, these tumors preserve overall encapsulation.

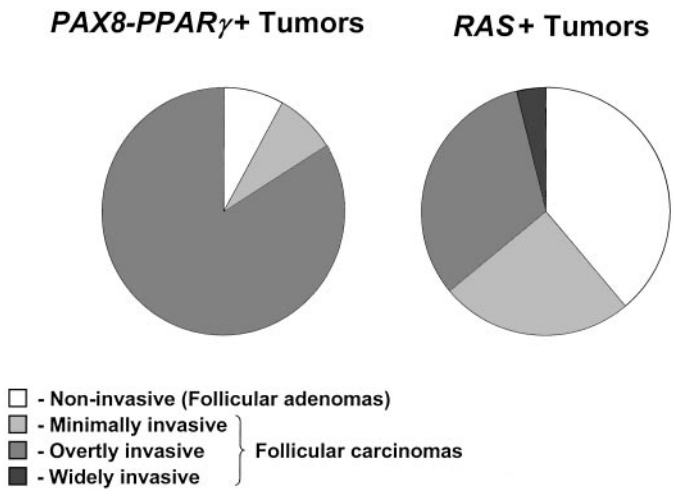

FIG. 4. Spectrum of invasiveness of follicular tumors with *PPARγ* rearrangement and *RAS* mutations.

On the other hand, the *RAS+/PPARγ−* genotype was observed in almost equal number of follicular carcinomas and follicular adenomas (Fig. 4). The follicular adenomas displayed no morphologic indicators of malignancy and showed little expression of galectin-3 and some immunoreactivity for HBME-1. The follicular carcinomas demonstrated the entire spectrum of histologic invasiveness and were minimally, overtly, and widely invasive. This suggests that *RAS*-initiated follicular carcinomas develop through a benign follicular adenoma stage/precursor. Thus, RAS activation by itself appears insufficient to determine malignant growth but may predispose to acquisition of additional genetic or epigenetic alterations that lead to a fully transformed phenotype.

This possibility is supported by *in vitro* studies. Acute expression of mutant *H-RAS* in cultured normal human thyroid cells induces a period of rapid proliferation during which the cells exhibit a partially transformed phenotype but retain differentiation features (37, 38). Remarkably, after 15–25 population doublings, the cells stop growing and undergo senescence, despite undiminished expression of mutant RAS. This self-limited cell proliferation with the retention of differentiation properties recapitulates in many aspects the growth of human follicular adenomas. Indeed, thyroid-specific expression of mutant *K-RAS* in transgenic mice has shown to lead to the development of benign thyroid nodules and follicular adenomas, whereas carcinomas are rare and required additional goitrogen stimulation (39).

Hürthle cell carcinomas possess a distinct set of large-scale chromosomal abnormalities, as it has been demonstrated by comparative genomic hybridization and loss of heterozygosity studies (21, 40–42). Our data indicate that Hürthle cell adenomas and carcinomas have a very low frequency of either *RAS* mutations or *PAX8-PPARγ* rearrangement. These tumors, despite sharing some histologic features with conventional follicular tumors, apparently develop via separate molecular events and likely represent a distinct type of thyroid neoplasm.

Among unselected 17 follicular carcinomas in this study, 88% revealed either *RAS* (58%) or *PAX8-PPARγ* (30%) mutations. This suggests that molecular testing of thyroid FNA specimens may be useful to improve the accuracy of preoperative diagnosis of follicular tumors. Thus, finding of *PAX8-PPARγ* rearrangement in thyroid FNA samples would be a strong indicator of follicular carcinoma. As for *RAS* mutation, it cannot discriminate between follicular carcinoma and follicular adenoma but would allow distinction between follicular neoplasms and hyperplastic thyroid nodules. Such distinction is of considerable clinical importance because 42–77% of thyroid nodules removed surgically are nonneoplastic colloid nodules (2).

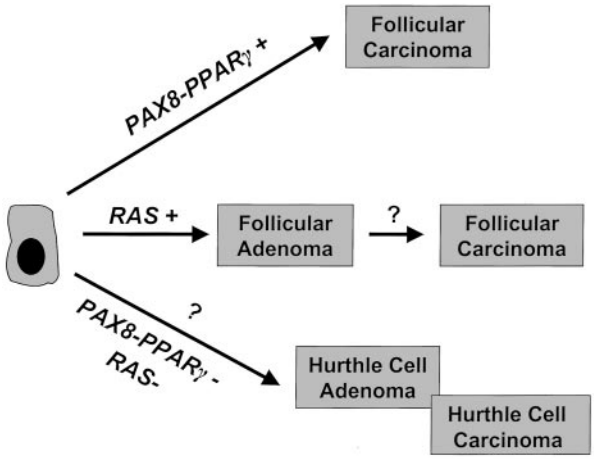

FIG. 5. Putative molecular pathways in thyroid conventional follicular and Hürthle cell tumors. Tumors harboring *PAX8-PPARγ* rearrangement directly develop as follicular carcinomas without a benign adenoma stage. Acquisition of *RAS* mutations leads to the development of follicular adenomas, whereas additional and still unknown genetic alterations require for malignant transformation and progression to a follicular carcinoma stage. Hürthle cell tumors lack both of these genetic alterations and require a separate set of mutations for their development. Whether Hürthle cell adenoma is a precursor lesion for Hürthle cell carcinoma remains unclear.

In conclusion, our data suggest that follicular thyroid carcinomas can develop through different molecular pathways (Fig. 5). For conventional follicular tumors, at least two distinct pathways exist, initiated by either *PAX8-PPARγ* rearrangement or *RAS* mutation. Hürthle cell tumors have a low frequency of both of these genetic alterations and apparently require a unique set of mutations for their development.

Acknowledgments

Received December 4, 2002. Accepted February 14, 2003.

Address all correspondence and requests for reprints to: Dr. Yuri Nikiforov, Department of Pathology, University of Cincinnati, 231 Albert Sabin Way, P.O. Box 670529, Cincinnati, Ohio 45267-0529. E-mail: yuri.nikiforov@uc.edu.

This work was supported by NIH Grants R01-CA88041 (to Y.N.) and CA75425 and a Georgia Cancer Coalition Distinguished Clinical Scientist Award (to T.G.K.). Tissue samples were collected in part using a support by a grant from the NIH (PHS M01 RR08084, the Children's Hospital–University of Cincinnati General Clinical Research Center Tissue Procurement Facility) and through the Cooperative Human Tissue Network (CHTN), which is funded by the National Cancer Institute.

References

1. **Hundahl SA, Fleming ID, Fremgen AM, Menck HR** 1998 A National Cancer Data Base report on 53,856 cases of thyroid carcinoma treated in the U.S., 1985–1995. Cancer 83:2638–2648
2. **Mazzaferri EL** 1993 Management of a solitary thyroid nodule. N Engl J Med 328:553–559
3. **Bartolazzi A, Gasbarri A, Papotti M, Bussolati G, Lucante T, Khan A, Inohara H, Marandino F, Orlandi F, Nardi F, Vecchione A, Tecce R, Larsson O** 2001 Application of an immunodiagnostic method for improving preoperative diagnosis of nodular thyroid lesions. Lancet 357:1644–1650
4. **Xu XC, el-Naggar AK, Lotan R** 1995 Differential expression of galectin-1 and galectin-3 in thyroid tumors. Potential diagnostic implications. Am J Pathol 147:815–822
5. **Gasbarri A, Martegani MP, Del Prete F, Lucante T, Natali PG, Bartolazzi A** 1999 Galectin-3 and CD44v6 isoforms in the preoperative evaluation of thyroid nodules. J Clin Oncol 17:3494–3502
6. **Chiariotti L, Berlingieri MT, De Rosa P, Battaglia C, Berger N, Bruni CB, Fusco A** 1992 Increased expression of the negative growth factor, galactoside-binding protein, gene in transformed thyroid cells and in human thyroid carcinomas. Oncogene 7:2507–2511
7. **Miettinen M, Karkkainen P** 1996 Differential reactivity of HBME-1 and CD15 antibodies in benign and malignant thyroid tumours. Preferential reactivity with malignant tumours. Virchows Arch 429:213–219
8. **Sack MJ, Astengo-Osuna C, Lin BT, Battifora H, LiVolsi VA** 1997 HBME-1 immunostaining in thyroid fine-needle aspirations: a useful marker in the diagnosis of carcinoma. Mod Pathol 10:668–674
9. **Cheung CC, Ezzat S, Freeman JL, Rosen IB, Asa SL** 2001 Immunohistochemical diagnosis of papillary thyroid carcinoma. Mod Pathol 14:338–342
10. **Lloyd RV** 2001 Distinguishing benign from malignant thyroid lesions: galectin 3 as the latest candidate. Endocr Pathol 12:255–257
11. **Nascimento MC, Bisi H, Alves VA, Longatto-Filho A, Kanamura CT, Medeiros-Neto G** 2001 Differential reactivity for galectin-3 in Hurthle cell adenomas and carcinomas. Endocr Pathol 12:275–279
12. **Herrmann ME, LiVolsi VA, Pasha TL, Roberts SA, Wojcik EM, Baloch ZW** 2002 Immunohistochemical expression of galectin-3 in benign and malignant thyroid lesions. Arch Pathol Lab Med 126:710–713
13. **Lemoine NR, Mayall ES, Wyllie FS, Williams ED, Goyns M, Stringer B, Wynford-Thomas D** 1989 High frequency of ras oncogene activation in all stages of human thyroid tumorigenesis. Oncogene 4:159–164
14. **Suarez HG, du Villard JA, Severino M, Caillou B, Schlumberger M, Tubiana M, Parmentier C, Monier R** 1990 Presence of mutations in all three ras genes in human thyroid tumors. Oncogene 5:565–570
15. **Esapa CT, Johnson SJ, Kendall-Taylor P, Lennard TW, Harris PE** 1999 Prevalence of Ras mutations in thyroid neoplasia. Clin Endocrinol (Oxf) 50:529–535
16. **Motoi N, Sakamoto A, Yamochi T, Horiuchi H, Motoi T, Machinami R** 2000 Role of ras mutation in the progression of thyroid carcinoma of follicular epithelial origin. Pathol Res Pract 196:1–7
17. **Lemoine NR, Mayall ES, Wyllie FS, Farr CJ, Hughes D, Padua RA, Thurston V, Williams ED, Wynford-Thomas D** 1988 Activated ras oncogenes in human thyroid cancers. Cancer Res 48:4459–4463
18. **Basolo F, Pisaturo F, Pollina LE, Fontanini G, Elisei R, Molinaro E, Iacconi P, Miccoli P, Pacini F** 2000 N-ras mutation in poorly differentiated thyroid carcinomas: correlation with bone metastases and inverse correlation to thyroglobulin expression. Thyroid 10:19–23
19. **Namba H, Rubin SA, Fagin JA** 1990 Point mutations of ras oncogenes are an early event in thyroid tumorigenesis. Mol Endocrinol 4:1474–1479
20. **Schark C, Fulton N, Jacoby RF, Westbrook CA, Straus 2nd FH, Kaplan EL** 1990 N-ras 61 oncogene mutations in Hurthle cell tumors. Surgery 108:994–1000
21. **Tallini G, Hsueh A, Liu S, Garcia-Rostan G, Speicher MR, Ward DC** 1999 Frequent chromosomal DNA unbalance in thyroid oncocytic (Hurthle cell) neoplasms detected by comparative genomic hybridization. Lab Invest 79: 547–555
22. **Kroll TG, Sarraf P, Pecciarini L, Chen CJ, Mueller E, Spiegelman BM, Fletcher JA** 2000 PAX8-PPARgamma1 fusion oncogene in human thyroid carcinoma. Science 289:1357–1360
23. **Nikiforova MN, Biddinger PW, Caudill CM, Kroll TG, Nikiforov YE** 2002 PAX8-PPARgamma rearrangement in thyroid tumors: RT-PCR and immunohistochemical analyses. Am J Surg Pathol 26:1016–1023
24. **Marques AR, Espadinha C, Catarino AL, Moniz S, Pereira T, Sobrinho LG, Leite V** 2002 Expression of PAX8-PPAR gamma 1 rearrangements in both follicular thyroid carcinomas and adenomas. J Clin Endocrinol Metab 87:3947–3952
25. **French CA, Alexander EK, Cibas ES, Nose V, Faquin W, Garber J, Moore F, Fletcher JA, Larsen P, Kroll TG,** Genetic and biologic subgroups of early stage follicular thyroid cancer. Am J Pathol, in press
26. **Martelli ML, Iuliano R, Le Pera I, Sama I, Monaco C, Cammarota S, Kroll T, Chiariotti L, Santoro M, Fusco A** 2002 Inhibitory effects of peroxisome proliferator-activated receptor gamma on thyroid carcinoma cell growth. J Clin Endocrinol Metab 87:4728–4735
27. **Rosai J, Carcangiu ML, DeLellis RA** 1992 Tumors of the thyroid gland. Atlas of tumor pathology. Washington: Armed Forces Institute of Pathology
28. **LiVolsi VA** 1990 Surgical pathology of the thyroid. Philadelphia: WB Saunders Co.
29. **Nikiforov YE, Nikiforova MN, Gnepp DR, Fagin JA** 1996 Prevalence of mutations of ras and p53 in benign and malignant thyroid tumors from children exposed to radiation after the Chernobyl nuclear accident. Oncogene 13:687–693
30. **Nikiforova MN, Caudill CM, Biddinger P, Nikiforov YE** 2002 Prevalence of RET/PTC rearrangements in Hashimoto's thyroiditis and papillary thyroid carcinomas. Int J Surg Pathol 10:15–22
31. **Argani P, Zakowski MF, Klimstra DS, Rosai J, Ladanyi M** 1998 Detection of the SYT-SSX chimeric RNA of synovial sarcoma in paraffin-embedded tissue and its application in problematic cases. Mod Pathol 11:65–71
32. **Elenitoba-Johnson KS, Bohling SD, Wittwer CT, King TC** 2001 Multiplex PCR by multicolor fluorimetry and fluorescence melting curve analysis. Nat Med 7:249–253
33. **Nakao M, Janssen JW, Seriu T, Bartram CR** 2000 Rapid and reliable detection of N-ras mutations in acute lymphoblastic leukemia by melting curve analysis using LightCycler technology. Leukemia 14:312–315

34. **Wittwer CT, Herrmann MG, Moss AA, Rasmussen RP** 1997 Continuous fluorescence monitoring of rapid cycle DNA amplification. Biotechniques 22: 130–131, 134–138
35. **Lynch RA, Wagoner L, Li S, Sparks L, Molkentin J, Dorn 2nd GW** 2002 Novel and nondetected human signaling protein polymorphisms. Physiol Genomics 10:159–168
36. **Roque L, Castedo S, Clode A, Soares J** 1993 Deletion of 3p25–>pter in a primary follicular thyroid carcinoma and its metastasis. Genes Chromosomes Cancer 8:199–203
37. **Lemoine NR, Staddon S, Bond J, Wyllie FS, Shaw JJ, Wynford-Thomas D** 1990 Partial transformation of human thyroid epithelial cells by mutant Ha-ras oncogene. Oncogene 5:1833–1837
38. **Jones CJ, Kipling D, Morris M, Hepburn P, Skinner J, Bounacer A, Wyllie FS, Ivan M, Bartek J, Wynford-Thomas D, Bond JA** 2000 Evidence for a telomere-independent "clock" limiting RAS oncogene-driven proliferation of human thyroid epithelial cells. Mol Cell Biol 20:5690–5699
39. **Santelli G, de Franciscis V, Portella G, Chiappetta G, D'Alessio A, Califano D, Rosati R, Mineo A, Monaco C, Manzo G, et al.** 1993 Production of transgenic mice expressing the Ki-ras oncogene under the control of a thyroglobulin promoter. Cancer Res 53:5523–5527
40. **Segev DL, Saji M, Phillips GS, Westra WH, Takiyama Y, Piantadosi S, Smallridge RC, Nishiyama RH, Udelsman R, Zeiger MA** 1998 Polymerase chain reaction-based microsatellite polymorphism analysis of follicular and Hurthle cell neoplasms of the thyroid. J Clin Endocrinol Metab 83:2036–2042
41. **Zedenius J, Wallin G, Svensson A, Grimelius L, Hoog A, Lundell G, Backdahl M, Larsson C** 1995 Allelotyping of follicular thyroid tumors. Hum Genet 96:27–32
42. **Grebe SK, McIver B, Hay ID, Wu PS, Maciel LM, Drabkin HA, Goellner JR, Grant CS, Jenkins RB, Eberhardt NL** 1997 Frequent loss of heterozygosity on chromosomes 3p and 17p without VHL or p53 mutations suggests involvement of unidentified tumor suppressor genes in follicular thyroid carcinoma. J Clin Endocrinol Metab 82:3684–3691